MABS
2016, VOL. 8, NO. 7, 1276–1285
http://dx.doi.org/10.1080/19420862.2016.1214785

Taylor & Francis
Taylor & Francis Group

REPORT

OPEN ACCESS

Comparing domain interactions within antibody Fabs with kappa and lambda light chains

Raheleh Toughiri*, Xiufeng Wu, Diana Ruiz, Flora Huang, John W. Crissman, Mark Dickey, Karen Froning, Elaine M. Conner, Thomas P. Cujec, and Stephen J. Demarest

Eli Lilly and Company, Lilly Biotechnology Center, San Diego, CA, USA

ABSTRACT

IgG antibodies are multi-domain proteins with complex inter-domain interactions. Human IgG heavy chains (HCs) associate with light chains (LCs) of the κ or λ isotype to form mature antibodies capable of binding antigen. The HC/LC interaction involves 4 domains: VH and CH1 from the HC and VL and CL from the LC. Human Fabs with κ LCs have been well characterized for their unfolding behaviors and demonstrate a significant level of cooperativity and stabilization when all 4 domains are intact. Very little is known regarding the thermodynamic properties of human Fabs with λ LCs. Here, we dissect the domain contributions to Fab stability for both κ and λ LC-containing Fabs. We find the cooperativity of unfolding between the constant domains, CH1/Cλ, and variable domains, VH/Vλ, within λ LC-containing Fabs is significantly weaker than that of κ LC-containing Fabs. The data suggests there may not be an evolutionary necessity for strong variable/constant domain cooperativity within λ LC-containing Fabs. After investigating the biophysical properties of Fabs with mismatched variable and constant domain subunits (e.g., VH/Vκ paired with CH1/Cλ or T cell receptor Cα/Cβ), the major role of the constant domains for both κ- and λ-containing Fabs may be to reduce the hydrophobic exposure at the VH/VL interface. Even though Fabs with these non-native pairings were thermodynamically less stable, they secreted well from mammalian cells as well behaved monodisperse proteins, which was in contrast to what was observed with the VH/Vκ and VH/Vλ scFvs that secreted as a mixture of monomer and aggregates.

Abbreviations: One-anilino-8-naphthalene sulfonate, ANS; antibody complementarity-determining regions, CDRs; antibody fragment antigen binding, Fab; antibody variable domain fragment (VH/VL), Fv; circular dichroism, CD; differential scanning calorimetry, dithiothreitol, DTT; differential scanning calorimetry, DSC; ethylenediaminetetracetic acid, EDTA; first heavy chain constant domain, CH1; guanidinium hydrochloride, GuHCl; heavy chain, HC; immunoglobulin γ isotype, IgG; kappa constant domain, Cκ; lambda constant domain, Cλ; light chain, LC; midpoint of thermal unfolding, T_m; phosphate-buffered saline, PBS; single chain Fv, scFv; size exclusion chromatography, SEC; sodium dodecyl sulfate polyacrylamide gel electrophoresis, SDS-PAGE; T cell receptor, TCR; variable heavy chain domains, VH; variable kappa domain, Vκ; variable lambda domain, Vλ; variable light chain domain (general), VL

ARTICLE HISTORY
Received 17 March 2016
Revised 29 June 2016
Accepted 12 July 2016

KEYWORDS
Antibody; Fab; kappa light chain; lambda light chain; stability

Introduction

Immunoglobulins or antibodies are heterotetrameric glycoproteins essential to the vertebrate immune response. Immunoglobulins of the γ isotype (IgGs) are composed of 2 identical light chains (LCs) of either κ or λ isotype and 2 identical IgG heavy chains (HCs). The most prevalent isotype found in human serum, IgGs are also commonly used as therapeutics, with >30 monoclonal IgGs approved for therapeutic use in a wide range of indications.[1] The domain architecture of IgGs is complex, and includes both V- and C-class Ig-fold domains.[2] The V-class Ig-fold domains of the HC and LC (VH and VL, respectively) are responsible for the immense diversity that allows the immune system to generate an adaptive immune response to eliminate pathogens. The variable domains are a combination of a myriad of V, D and J (VH) or V and J (VL) gene elements, and are paired with one another to provide improved diversity. Upon immune stimulation, these domains undergo hypersomatic mutation directing their affinity toward a particular antigen. The V-genes are spliced with the constant (C-class Ig-fold) HC and LC genes, and the full HC and LC proteins are expressed, assembled via chaperones and secreted by immune B cells.[3]

Once assembled, IgGs have the well-known 'Y' shape comprising 2 Fab (antigen-binding fragment) moieties consisting of the HC/LC pairing region that are the antibody 'arms' and the Fc (fragment crystallizable) moiety consisting of the HC homodimerization/FcγR binding region that is the 'stalk'. The Fab and Fc regions are distinct globular protein units separated by a flexible hinge region with little to no noncovalent interactions between them.[4,5] Once assembled, both the Fab and Fc regions are disulfide-linked dimers (hetero- and homodimer, respectively) with uncommonly high solubility and thermal stability

CONTACT Stephen J. Demarest demarestsj@lilly.com Lilly Biotechnology Center, 10300 Campus Point Drive, San Diego, CA 92130, USA
*Current address: Sorrento Therapeutics, San Diego, CA, USA

properties compared to most other human proteins.[5] The general high stability/solubility contributes to long-term plasma residency and their utility as therapeutics. This is not to suggest that stability/solubility fallibilities have not been observed for monoclonal IgGs when pushed to manufacturing and formulations extremes.[6]

The folding and stability of Fabs is complex and highly inter-domain dependent with a strong cooperativity. The CH1 domain within the Fab HC, is intrinsically unfolded in isolation and binds to the BiP chaperone, requiring LC binding for chaperone release and antibody secretion.[3] Most biophysical studies with Fabs have focused on IgG heavy chains associated with κ light chains.[7] Perhaps the most comprehensive study of the inter-domain interactions within Fabs was provided by Röthlisberger et al., who performed a dissection of the energetics of predominately murine Fabs with varied VH and VL thermal stability and showed that the VH/Vκ and CH1/Cκ heterodimeric subunits significantly stabilize one another not through specific non-covalent interactions between the VH/CH1 interface or the Vκ/Cκ interface, where inter-domain interactions are sparse, but by acting as ideal linkers to stabilize each heterodimeric interface (VH/Vκ and CH1/Cκ) kinetically.[8] Where the VH/Vκ domains are stability limiting, addition of CH1/Cκ subunits can increase their thermal unfolding midpoints (T_m) by as much as 15–25 °C.[7,9] In κ LC Fabs with low variable domain stabilities, variable domains can unfold first, while in Fabs with very stable variable domains, CH1/Cκ can unfold first.[5,8,10] However, most κ LC Fabs contain moderately stable variable domains that unfold cooperatively with CH1/Cκ within the T_m range of 70–80 °C.[7,8,10,11]

We wished to expand what we know of the domain interactions within Fabs, in particular the relationship between the VH/VL subunits and CH1/CL subunits. The thermodynamic relationship between VH/Vλ and CH1/Cλ is much less studied than that of VH/Vκ and CH1/Cκ, even though immunoglobulins containing λ LCs are of similar prevalence as those with κ LCs in humans.[12] Interestingly, the extracellular region of α/β T-cell receptors (TCRs) maintain a heterodimeric structure similar to antibody Fabs,[13] with both the TCRα and TCRβ chains consisting of N-terminal V-genes and C-terminal C-class domains (Fig. 1). Like antibody Fabs, the TCR heterodimer is stabilized by an inter-chain disulfide at the C-terminus of the C-class domains before membrane insertion. In this study, we generate Fabs with both native and non-native V-gene and C-gene pairings (Fig. 1) and characterize their unfolding properties to compare inter-domain subunit cooperativity within antibody Fabs of different light chain and overall constant domain composition.

Results

Generation of Fabs with varied VH/VL and CH1/CL subunit combinations

Single domain constructs Cκ and Cλ, scFv constructs from pertuzumab[14] and PGT128[15,16] (with VH/Vκ and VH/Vλ pairings, respectively), heterodimeric constant domain subunit constructs IgG1 CH1/Cκ and CH1/Cλ, and various fully Fab constructs using the pertuzumab and PGT128 VH/VL subunits were produced to evaluate the thermodynamic relationships of different isotypes of V-genes and C-genes (Table 1). Constructs containing the TCR Cα/Cβ domains were engineered to have optimized HC/LC association based on optimized V-gene/C-gene linker regions including an FG loop replaced with a

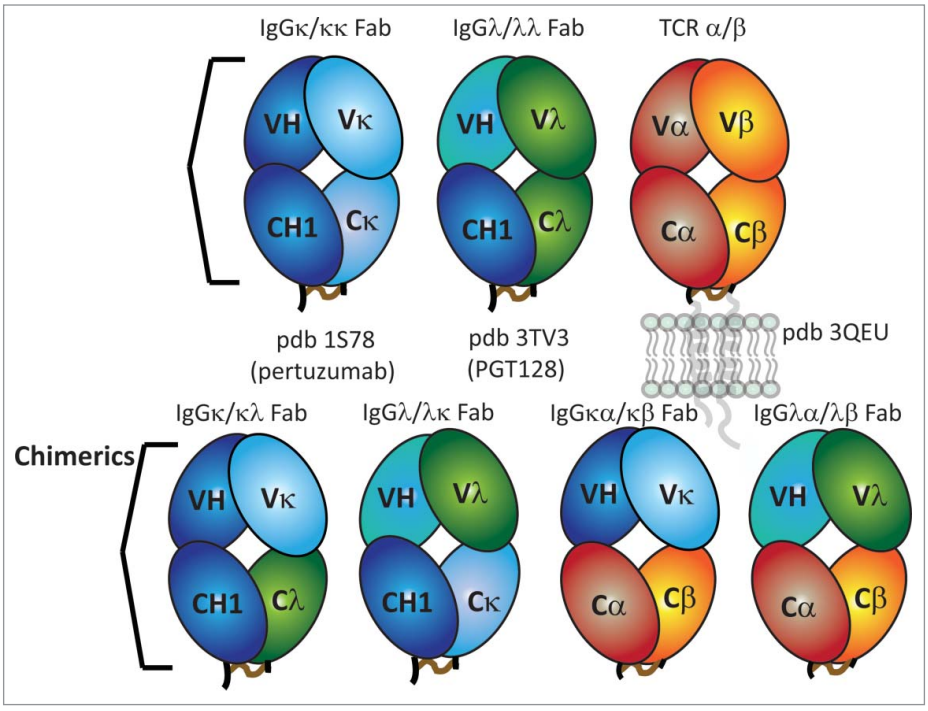

Figure 1. Schematic diagrams of Fab constructs produced to evaluate cooperative inter-domain interactions within antibody Fabs. On top, are wild-type Fab and T cell receptor diagrams. All three proteins comprise a similar structure with 2 V-class domains responsible for antigen binding and 2 C-class domains linked by a C-terminal inter-chain disulfide bond. For the study described here, we utilized pertuzumab (pdb 1S78) as a representative κ LC Fab and PGT128 (pdb 3TV3) as a representative λ LC Fab. On the bottom, are schematics of the chimeric Fabs that were generated to evaluate the thermodynamic properties of variable and constant domains within Fabs.

Table 1. Compendium of single domain, VH/VL subunit, CH1/CL subunit, and full Fab constructs that were expressed and purified for characterization.

LC constant domains and CH1/CL heterodimers	Constructs containing Pertuzumab VH/Vκ	Constructs containing PGT128 VH/Vλ
Cκ	scFv-Fc[a]	scFv-histag
Cλ	VHCH1/VκCκ	VHCH1/VλCλ
IgG1_CH1/Cκ	VHCH1/VκCλ	VHCH1/VλCκ
IgG1_CH1/Cλ	VHCα/VκCβ	VHCα/VλCβ

[a]Isolated scFv was too unstable to be produced without being a fusion protein to an IgG1 Fc.

canonical type II' β-turn.[17] Both scFv constructs were generated in the VH/VL format with a flexible $(G_4S)_4$ linker. All constructs contained C-terminal histidine tags; for HC/LC heterodimers, the histags were placed at the C-terminus of the HC following the cysteine that forms the inter-chain disulfide. The pertuzumab scFv expressed poorly as a highly heterogeneous protein of multiple-sized aggregates and could only be produced in a predominately monodisperse form as an N-terminal Fc fusion protein. All proteins except the pertuzumab scFv-Fc and PGT128 scFv could be purified to >90% monomeric purity using an affinity chromatography step with or without an initial ion exchange capture step (see Fig. 2 for SDS-PAGE and analytical size-exclusion chromatography (SEC) with the pertuzumab VH/Vκ-containing Fabs). Molecular weights were additionally confirmed using static light scattering attached in-line to the analytical SEC column. The Fabs containing Cα/Cβ were clearly glycosylated based on their higher apparent molecular weight by SEC and broader staining pattern on SDS-PAGE. Cα and Cβ contain 3 and 1 N-linked glycosylation motifs, respectively. Incubation with N-glycanase can clearly reduce the apparent hydrodynamic radius of the Fabs containing Cα/Cβ (Fig. 2B), although not quite to the same apparent size as the other Fabs.

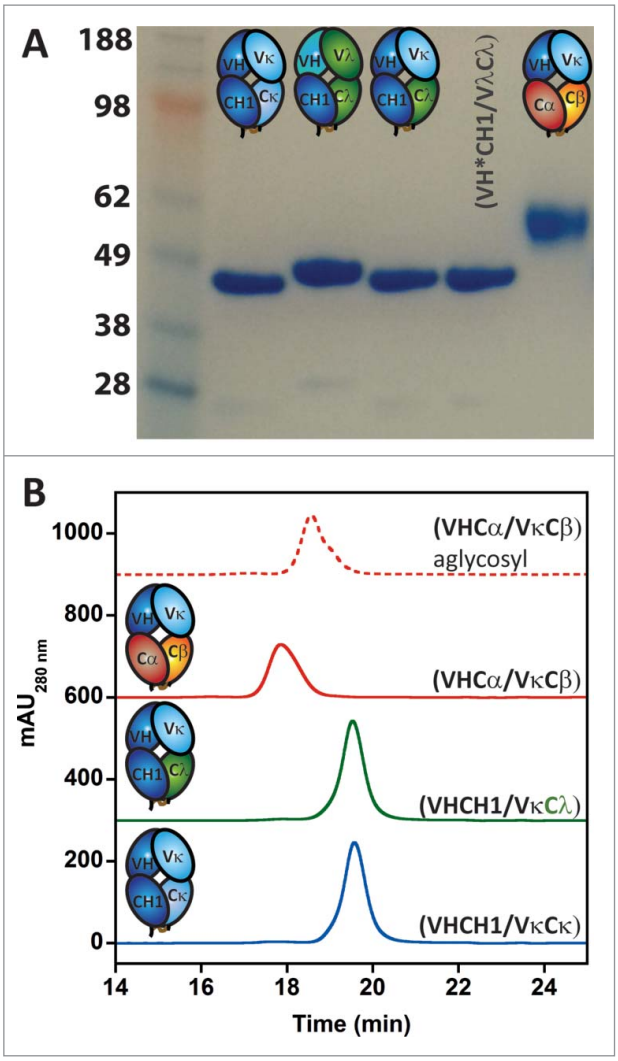

Figure 2. Representative SDS-PAGE and analytical size exclusion chromatography (SEC) of Fab constructs. (A) Non-reducing SDS-PAGE with the wild-type pertuzumab and PGT128 Fabs (lanes 2 and 3, respectively) and pertuzumab Fabs containing Cλ (lane 4) and Cα/Cβ (lane 6). Lane 5 contains a chimeric Fab with the pertuzumab HC and PGT128 LC. (B) Analytical SEC with in-line static light scattering confirmed the monodisperse nature of the constructs evaluated in this report. Shown are chromatograms of the wild-type pertuzumab Fab (bottom), pertuzumab Fab containing Cλ, and containing Cα/Cβ. The uppermost chromatogram is of the Cα/Cβ-containing pertuzumab Fab after enzymatic N-linked glycan removal.

Differential scanning calorimetry of isolated Cκ and Cλ domains and CH1/Cκ and CH1/Cλ subunits

To fully understand the inter-domain interactions within the Fabs we generated, it was important to have benchmark measurements with the constant domains (Cκ and Cλ) and heterodimeric constant domain subunits (CH1/Cκ and CH1/Cλ) in isolation. We elected to perform differential scanning calorimetry (DSC) to take advantage of the technique's ability to discriminate complex, multi-domain unfolding events (typical for immunoglobulins) due to the derivative nature of the thermal unfolding data and ability to experimentally measure $\Delta H_{unfolding}$.[18] When studied by DSC, both Cκ and Cλ demonstrate single and reversible thermal unfolding curves (albeit 30% reduced ΔH_{cal} for Cλ upon cooling and reheating). The midpoints of thermal denaturation (T_ms) were low (58–59 °C) compared to what has generally been observed for intact Fabs.[5] IgG1 CH1 did not express in isolation. This is not surprising given that it is known to be intrinsically unfolded in isolation.[19] The CH1/Cκ and CH1/Cλ subunits, however, did express well in the *E. coli* periplasm or when secreted from mammalian cells as heavy chain fusions to IgG1-Fc. DSC experiments with the heterodimers showed a significant increase in thermal stability for both Cκ and Cλ upon complexing with CH1 (Fig. 3A, 4A, Table 2). Neither subunit showed any trace of reversibility after thermal denaturation, suggesting the presence of the CH1 domain likely induces aggregation/precipitation. Some variable domains demonstrate reversible unfolding in isolation,[20] but Fabs generally do not.[5] This suggests the CH1 domain as the limiting factor for the refoldability of IgG Fabs in general.

Investigation of inter-domain interactions within a κ LC Fab

We next investigated the inter-domain energetics within the pertuzumab Fab that naturally has a κ LC. Thermal unfolding by DSC of the wild-type pertuzumab Fab compared to the individual VH/Vκ and CH1/Cκ subunits demonstrated the typical large increase in both stability and cooperativity that is often observed when combining the variable and constant domain

subunits within κ LC-containing Fabs (Fig. 3A).[8,11] Within the scFv, one domain was clearly less stable and was identified below as VH. As a native-like Fab consisting of all 4 domains, VHCH1/VκCκ, all the domains are stabilized to the extent that they unfold cooperatively as a single unit. This results in a large (+21°C) increase in the VH T_m and modest increases in T_m for Vκ and the CH1/Cκ subunit (Table 2). It is generally the least stable domain of a complex that benefits most thermodynamically from protein-protein interactions.[9]

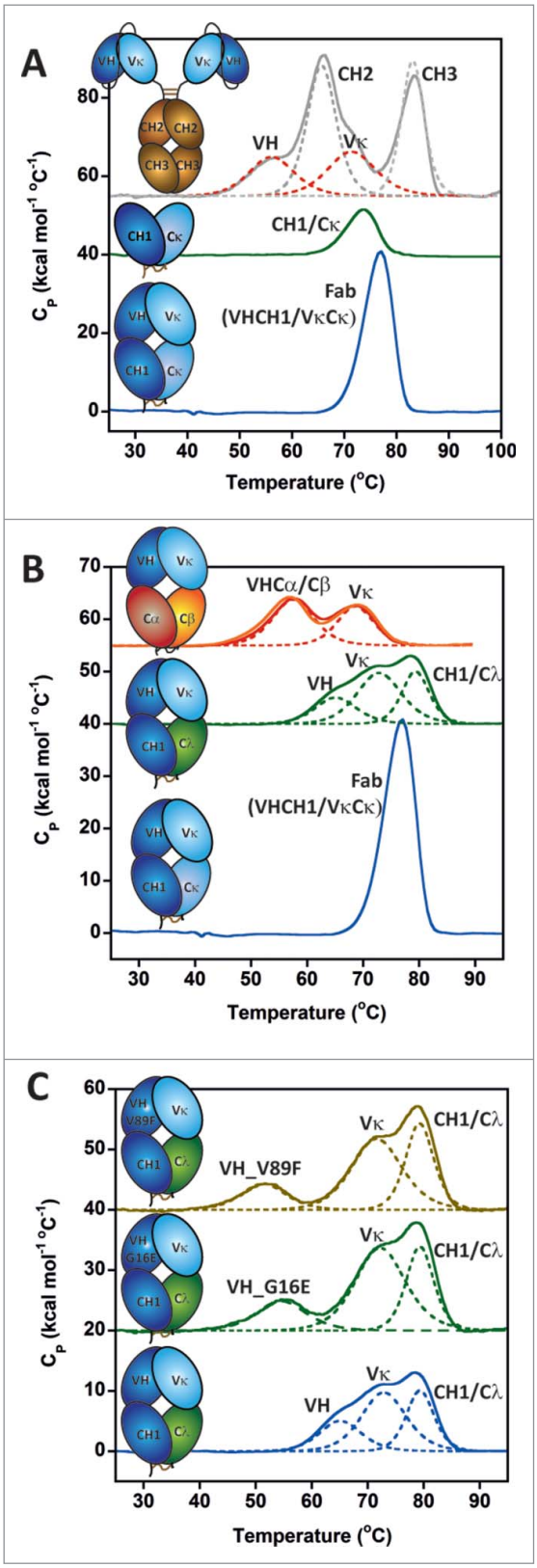

We next evaluated the specific ability of the CH1/Cκ subunit to promote such a dramatic increase in Fab stability when paired with VH/Vκ. In their 2005 report, Röthlisberger and coworkers describe that the stabilization of the individual VH/Vκ and CH1/Cκ subunits is likely not the result of non-covalent stabilizing interactions between the V-genes and C-genes since this interface is quite small, but rather the result of a stronger overall interface between HC and LC, with each subunit acting as an ideal linker for one another, which stabilizes the HC/LC interface.[8] Based on this, we wished to learn how specific the CH1/Cκ subunit stabilization is to VH/Vκ subunits and whether related constant domain subunits could similarly stabilize the VH/Vκ subunit. The first and most obvious subunit to replace CH1/Cκ is CH1/Cλ. Structurally, Cκ and Cλ are similar and use similar residues to interact with antibody CH1 domains; however, the sequence homology is only 40%. We also evaluated replacing the entire CH1/Cκ subunit with the TCR Cα/Cβ subunit, which is structurally homologous and has been shown capable of pairing with VH/Vκ.[17]

DSC data with the native and chimeric Fab constructs clearly shows that the native and stabilizing pairing of CH1/Cκ with VH/Vκ is highly specific and not easily reproduced with structural homologues (Fig. 3B). The pertuzumab Fab containing Cλ instead of Cκ does experience some stabilization via the combination; the VH domain T_m increases by 9°C (Table 2), but unfolds at a temperature too low compared to the Vκ and CH1/Cλ subunit to observe cooperativity. We identified the VH domain as the domain of least stability by adding destabilizing mutations within VH and analyzing the resulting thermal unfolding profile (Fig. 3C). The Cλ-containing pertuzumab Fab secreted well from HEK293F cells as a well-behaved heterodimer of roughly 50 kDa, unlike the pertuzumab scFv, which expressed poorly and contained a high percentage of aggregates. Thus, while there is clearly a loss of cooperativity and stability within the multi-domain Fab complex when replacing Cκ with Cλ, the presence of CH1/Cλ reduces aggregation/misfolding that occurs within the Fv subunit lacking constant domains.

To further investigate differences in stability and cooperativity within the pertuzumab Fabs containing Cκ and Cλ, a guanidinium hydrochloride (GuHCl) denaturation was performed and monitored by circular dichroism (CD). There is a clear aromatic shoulder present in the far UV CD spectrum of the wild-type pertuzumab Fab that peaks at 234 nm and can be used to

Figure 3. Differential scanning calorimetry (DSC) evaluation of the thermal unfolding of the κ LC-containing pertuzumab Fab. (A) DSC traces of the pertuzumab Fab (bottom), CH1/Cκ subunit (middle), and VH/Vκ pertuzumab scFv (top). The pertuzumab scFv was not stable when expressed on its own, but did express fairly well as an N-terminal fusion to IgG1 Fc. (B) DSC traces of the wild-type pertuzumab Fab (bottom), Cλ-containing pertuzumab Fab (middle), and Cα/Cβ-containing pertuzumab Fab both before (red) and after (orange) enzymatic deglycosylation (top). (C) DSC traces of Cλ-containing pertuzumab Fab before (bottom) and after introduction of destabilizing VH mutations G16E (middle) or V89F (top). These mutations were made to determine whether VH or VL was the less stable of the pertuzumab variable domains. Clearly VH is the less stable of the two. For all DSC traces, the identity of the domain(s) giving rise to each transition is labeled.

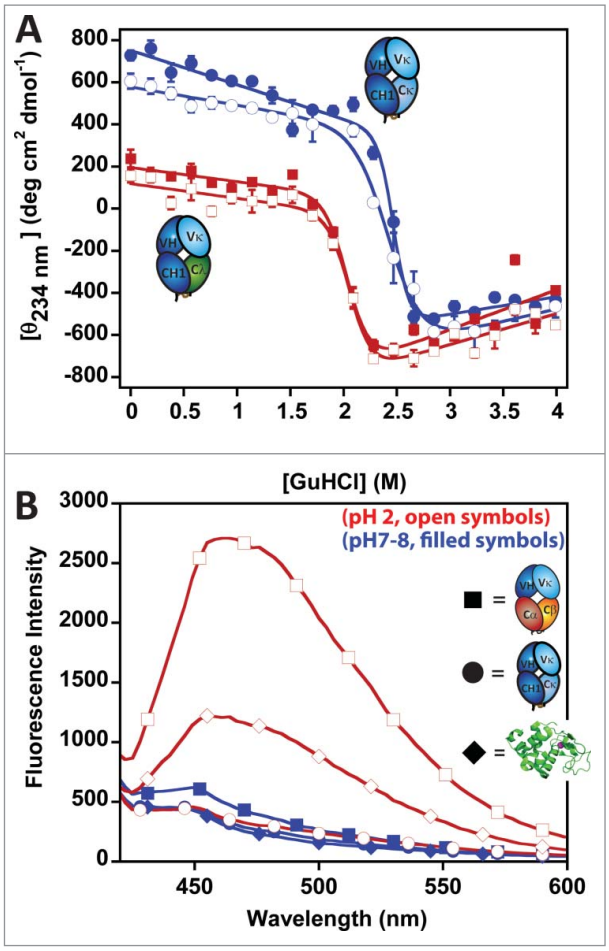

Figure 4. Guanidinium HCl (GuHCl) chemical denaturations and 1-anilino-8-naphthalene sulfonate (ANS) binding of the pertuzumab Fabs. (A) GuHCl denaturation of the wild-type pertuzumab Fab (blue circles) and Cλ-containing pertuzumab Fab (red squares) at 1 mg/mL (open symbols) and 2 mg/mL (closed symbols). Only one transition was visible by Far UV circular dichroism (CD) at 234 nm; therefore, the curves were fit to a single unfolding event to obtain the *m*-value (slope of denaturation), which is correlated with the change in solvent exposed surface area for protein unfolding,[30] and the GuHCl concentration where 50% of the protein is unfolded (C_{50}). (B) ANS fluorescence in the presence of the wild-type pertuzumab Fab (circles), Cα/Cβ-containing pertuzumab Fab (squares) in PBS buffer (blue closed symbols) and under acidic conditions (red open symbols). The protein α-lactalbumin was used as both a negative and positive control (diamonds). α-lactalbumin should not bind and induce fluorescence of ANS at neutral pH bound to Ca^{2+} (pH 8, 500 mM $CaCl_2$), but is known to partially unfold and bind ANS under acidic conditions (< pH 3).

monitor unfolding (Fig. 4A). This shoulder is present, but slightly reduced in intensity in the Cλ-containing pertuzumab Fab, possibly due to destabilization/modification of the structural environment of the aromatic residue(s) that give(s) rise to the peak. Although the DSC thermal unfolding data clearly shows 3 separate unfolding events for the Cλ-containing Fab, only one unfolding transition is visible in the GuHCl denaturation monitored by the far UV CD signal. In agreement with the DSC data, the folded state of the Cλ-containing pertuzumab Fab is less stable when fit to a 2-state denaturation curve (WT Fab $\Delta G_U°(20\,°C) = +62$ kJ/mol; Cλ Fab = +49 kJ/mol; Fig. 4A). The *m*-value (slope of the unfolding transition) was slightly lower for the Cλ-containing Fab if the fit values from both 1 and 2 mg/mL experiments are averaged, although not as much as expected based on the DSC data. If only the higher sensitivity 2 mg/mL data is used, the *m*-value of the wild-type pertuzumab Fab is roughly twice that of the Fab containing Cλ.

We next paired the Cα/Cβ subunit with the pertuzumab VH/Vκ subunit to determine the effect of pairing entirely different variable and constant domain subunits. The DSC data indicates that this pairing only marginally changed the apparent VH/Vκ thermal stability (VH $T_m = +3\,°C$ over that of the scFv, Table 2). The Cα/Cβ-containing pertuzumab Fab did express well with much less intrinsic aggregation than the scFv or scFv-Fc. Together, the CH1/Cλ and Cα/Cβ additions to the pertuzumab VH/Vκ, have a positive effect on the monomeric behavior of the Fab compared to the scFv, perhaps by limiting the overall dynamics of the VH/Vκ and the exposure of hydrophobic surface area that is buried at the interface.

The Cα/Cβ subunit appears to be significantly less stable than isolated CH1/Cκ or CH1/Cλ. The unfolding transition may occur at the same temperature as the pertuzumab VH domain (Fig. 3B); the ratio of the calorimetrically measured $\Delta H_U°(T)$ values (area under the curve) for VH versus Vκ shifted compared to what was observed with the pertuzumab scFv alone (Fig. 3A,B), indicating the possible presence of an additional unfolding transition. With only the potential observation of a Cα/Cβ unfolding transition by DSC, we considered whether the Cα/Cβ subunit is not fully folded within the chimeric Fab, but in a partially unfolded state. Many crystal structures of Cα/Cβ show large areas of irregular secondary structure within the Cα domain with a surprising number of unsatisfied backbone hydrogen bonds.[21,22] We incubated the wild-type and Cα/Cβ-containing pertuzumab Fabs

Table 2. T_m values by DSC of the various Fab domains with and without VH/VL and CH1/CL coupling.

	Tm (°C), scFv-Fc	Tm, °C +CH1/Cκ	Tm, °C + CH1/Cλ	Tm, °C + Cα/Cβ
Pertuzumab VH/Vκ				
VH	56	77 (+21 °C)	65 (+9 °C)	59 (+3 °C)[a]
Vκ	71	77 (+6 °C)	73 (+2 °C)[b]	67 (−4 °C)
PGT128 VH/Vλ	Tm, °C scFv-histag	Tm, °C +CH1/Cκ	Tm, °C + CH1/Cλ	Tm, °C + Cα/Cβ
VH	63 (cooperative)	65 (+2 °C)[b]	68 (+6 °C)	64 (+1 °C)[b]
Vλ	63 (cooperative)	65 (+2 °C)[b]	68 (+6 °C)	64 (+1 °C)[b]
CH1/CL subunit	Tm, Cκ or Cλ isolated domain	Tm CH1/CL subunit	Tm, +VH/Vκ	Tm, +VH/Vλ
Cκ	59 (−15 °C)	74	77 (+3 °C)	69 (−5 °C)
Cλ	58 (−20 °C)	78	79 (+1 °C)[b]	79 (+1 °C)[b]

[a]Peak overlap with Cα/Cβ subunit likely makes this result indistinguishable from VH within the scFv.
[b]T_m differences of 1–2 °C in experiments performed over a few months period may be within the error.

with the hydrophobic dye ANS (1-anilinonaphthalene-8-sulfonate), which associates with partially folded proteins.[23] No ANS binding was observed for either Fab. The protein α-lactalbumin was used as a positive control because it is known to bind ANS under acidic conditions where it loses its binding capacity for Ca^{2+} and forms a partially unfolded state with significant α-helical content.[24] Only at pH 2.0 did the Cα/Cβ-containing Fab bind ANS, suggesting that a partially folded state could only be induced under non-native conditions. It seems unlikely that Cα/Cβ are fully unfolded at neutral pH given the large amount of exposed hydrophobic surface area that would be expected to induce aggregates, a trait that is not observed, and the fact that the Cα/Cβ inter-domain disulfide bond forms so readily. Thus, it does appear that the weak, but apparent overlapping peak in the DSC corresponds to the unfolding of the Cα/Cβ subunit.

Investigation of inter-domain interactions within a λ LC Fab

We next investigated the inter-domain interactions within a Fab (PGT128) that naturally contains a λ LC. DSC studies with the intact Fab compared to the VH/Vλ and CH1/Cλ subunits showed a very different trend than that observed for the pertuzumab Fab. The PGT128 VH/Vλ pair appeared to unfold cooperatively, whereas the unfolding events of the VH and Vκ of pertuzumab were clearly uncoupled (Fig. 5A). Combination of the much more stable CH1/Cλ subunit to the PGT128 VH/Vλ domains led to only a modest increase in the VH/Vλ T_m (+6 °C) compared to the large (+21 °C) VH T_m increase observed for pertuzumab (Fig. 5A, Table 2). Replacing the CH1/Cλ domains with either CH1/Cκ or Cα/Cβ did not significantly stabilize the PGT128 variable domains (Fig. 5B, Table 2). For the PGT128 Fab containing Cα/Cβ, a small broad peak with a T_m of ~50–55 °C was observed. This is likely the same peak observed for the pertuzumab Fab containing Cα/Cβ, which we associated with the unfolding of the Cα/Cβ subunit.

While there is published data to compare the unfolding properties of various κ LC-containing Fabs,[5,7] little has been published on Fabs that contain λ LCs. Was the non-cooperative folding of VH/Vλ and CH1/Cλ within the PGT128 Fab an anomaly or general feature of λ LC-containing Fabs? To address this, we generated 2 additional λ LC-containing Fabs for testing. The additional Fabs originated from pdbs 1NL0 (10C12 Fab) and 3THM (EP6b_B01 Fab).[25,26] Both Fabs expressed well as monodisperse proteins. DSC data showed that both Fabs had much higher thermal stability than PGT128 (Fig. 5C). Both had very high thermal stability, with T_ms greater than or equal to 6 °C the T_m (78 °C) observed for the CH1/Cλ subunit in isolation. The very large calorimetrically determined $\Delta H_U^\circ(T)$ observed for both the 10C12 and 3P6b_B01 Fabs (greater than was expected for the combination VH/Vλ subunit and CH1/Cλ subunits unfolding coincidentally at the same time without any cooperativity based on the PGT128), suggests some unfolding cooperativity when VH/Vλ and CH1/Cλ stabilities are near matched (Fig. 5C). There is a small shoulder on the left (lower temperature) side of the most stable Fab, 3P6b_B01, that may be the beginning of an uncoupling of VH/Vλ and CH1/Cλ; however, the CH1/Cλ is modestly stabilized compared to CH1/Cλ within PGT128 or the isolated CH1/Cλ

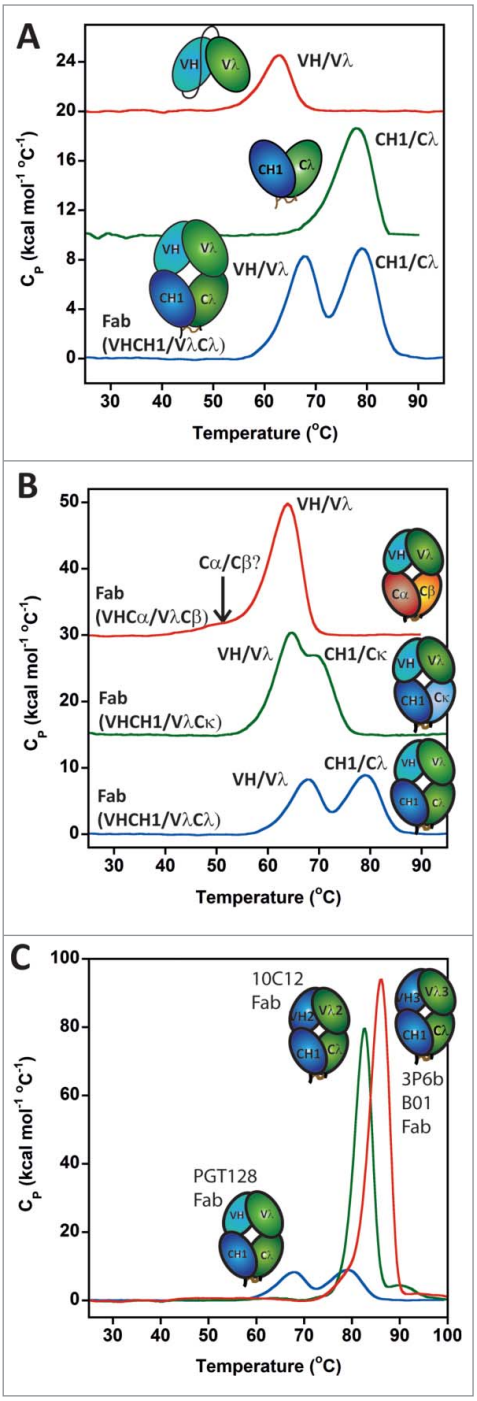

Figure 5. DSC evaluation of the thermal unfolding of the λ LC-containing PGT128 Fab. (A) DSC traces of the wild-type PGT128 Fab (bottom), CH1/Cλ subunit (middle), and VH/Vλ PGT128 scFv (top). (B) DSC traces of the wild-type PGT128 Fab (bottom), Cκ-containing PGT128 Fab (middle), and Cα/Cβ-containing PGT128 Fab (top). (C) DSC traces of the wild-type PGT128 Fab (blue), 10C12 Fab (green), and 3P6b_B01 Fab (red) all naturally containing fully λ LCs. For all DSC traces, the identity of the domain(s) giving rise to each transition are labeled.

subunit. We believe the small hump with a T_m of 90 °C for the 10C12 Fab is an artifact of imperfect baseline correction.

A thermal stability comparison of 6 matched scFv/Fab pairs from human antibodies with either κ or λ LCs

Given that we observed a striking difference in the cooperative folding within the Fab subunits of pertuzumab (κ LC) and

PGT128 (λ LC), we undertook an effort to demonstrate whether this result held true for additional Fabs with κ vs. λLCs. We obtained 6 human antibody sequences from an in-house source, 3 with κ LCs (denoted Antibody1κ-3κ) and 3 with λ LCs (denoted Antibody1λ-3λ). The antibodies were chosen to have diverse germline representation. For the κ LC antibodies, Antibody1κ had VH4/Vκ1 subfamilies; Antibody2κ had VH3/Vκ3 subfamilies; and Antibody3κ had VH1/Vκ1 subfamilies. For the λ LC antibodies, Antibody1λ had VH2/Vλ3 subfamilies; Antibody2λ had VH3/Vλ9 subfamilies; and Antibody3λ had VH1/Vλ2 subfamilies. We subcloned these into scFvs and Fabs, expressed them in mammalian cells and purified them using a single histag affinity chromatography step. All the proteins were predominately monodisperse except 'scFv1 (Vκ)', which was a mixture of monomer and higher-order aggregates (Fig. 6A, B). All scFvs except 'scFv1 (Vκ)' were found to be 27–28 kDa and all Fabs were found to be 47–50 kDa by static light scattering. The 'scFv1 (Vλ)' protein had a shoulder by SEC (Fig. 6B) potentially corresponding to incomplete signal peptide cleavage as judged by intact mass spectrometry.

We next performed DSC analyses on the human scFv and Fab proteins to evaluate further the cooperative folding properties of Fabs containing κ LCs versus those containing λ LCs. Two of the 3 scFvs containing Vκ domains, unfolded non-cooperatively, similar to the pertuzumab scFv (Fig. 6C). All three Fv regions experienced a dramatic increase in Tm in the Fab format, similar to what was observed for the pertuzumab Fab (Fig. 6C). Unlike the scFvs with Vκ, all 3 scFvs containing Vλ unfolded in a single apparent cooperative event, similar to the PGT128 scFv (Fig. 6D). Like the PGT128 Fab, the Fabs with λ LCs: 1) did not demonstrate cooperative unfolding of the Fvs and the CH1/Cλ subunits, and 2) did not have as dramatic increases in the Tm of the Fv when combined with CH1/Cλ in the Fab format (Fig. 6D). For Antibodyλ3, the Fv appeared to experience a *decrease* in Tm in the Fab format. Overall, there was a weak trend for the scFvs with Vκ to have lower Tms than those with Vλ (Table 3). Similar to the observations with pertuzumab (κ LC) and PGT128 (λ LC), there was strong inter-subunit cooperativity between VH/Vκ and CH1/Cκ that was much weaker for VH/Vλ and CH1/Cλ (Table 3).

Discussion

The studies described here highlight differences in the HC/LC inter-domain interactions mediated by κ and λ LC's. While the CH1/Cλ subunit itself is more stable than the CH1/Cκ subunit, CH1/Cλ does not impart the large inter-subunit cooperativity within an intact Fab that CH1/Cκ does (even when CH1/Cλ is natively paired with VH/Vλ). The CH1/Cλ domains do, however, improve the biophysical properties of the variable

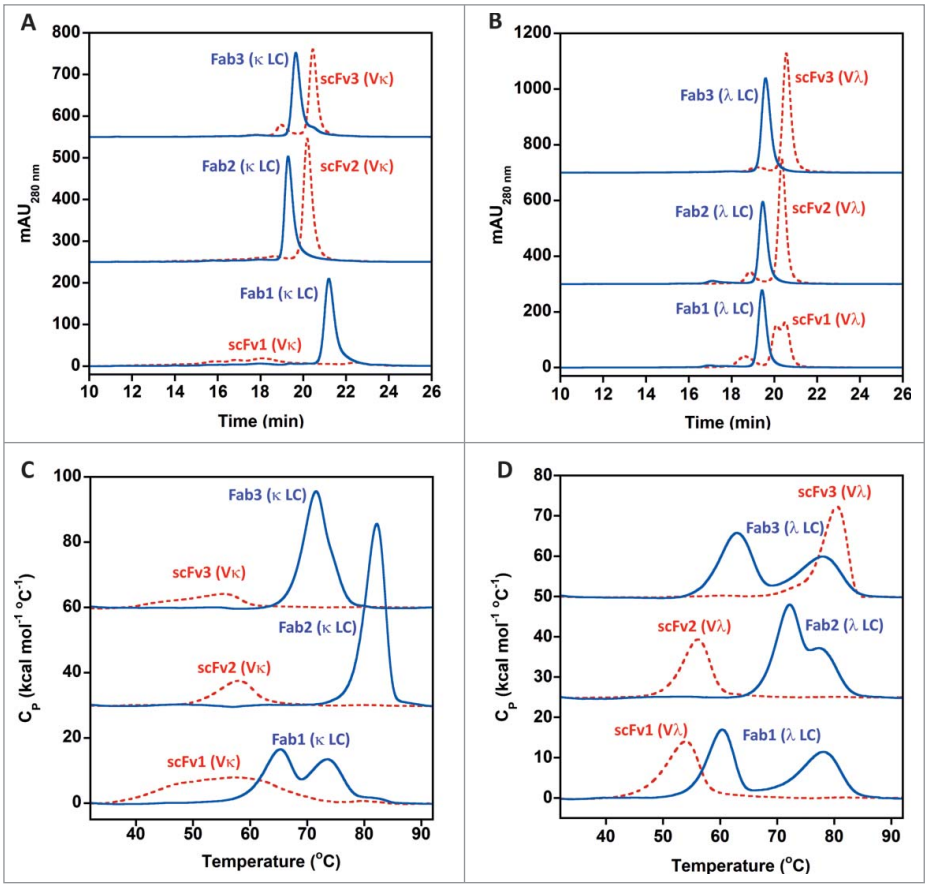

Figure 6. Comparison of 6 human scFvs and Fabs originating from antibodies with either κ or λ LCs. (A) Analytical SEC of matching scFvs and Fabs from 3 different human IgG1/κ mAbs. (B) Analytical SEC of matching scFvs and Fabs from 3 different human IgG1/λ mAbs. (C) DSC traces of matching scFvs and Fabs from 3 different human IgG1/κ mAbs. (D) DSC traces of matching scFvs and Fabs from 3 different human IgG1/λ mAbs.

Table 3. Comparing the thermal unfolding of human scFvs and Fabs with κ vs. λ LCs.

Antibody	Tm1 scFv (°C)	Tm1 Fab (°C)	ΔTm (°C)
Antibody1κ	48 (non-cooperative)[a]	65	+17
Antibody2κ	57 (cooperative)[a]	82	+25
Antibody3κ	47 (non-cooperative)[a]	71	+24
Average	51 ± 6	73 ± 9	+22 ± 4
Antibody1λ	53 (cooperative)[a]	60	+7
Antibody2λ	56 (cooperative)[a]	72	+16
Antibody3λ	80 (cooperative)[a]	63	−17
Average	63 ± 12[b]	66 ± 5[b]	+3 ± 14[b]

[a]Cooperative indicates that VH and VL unfold simultaneously while non-cooperative indicates one unfolds before the other. For the non-cooperative scFv unfolding, the lowest Tm value is listed.
[b]Data for PGT128 was averaged with the data from Antibody1λ-3λ as it was also a fully human antibody. Pertuzumab was left out of the average for Antibody1κ-3κ since it was humanized and the presence of mouse residues hypothetically could have an effect on the observations.

domains to which they are associated regardless of whether they are VH/Vκ or VH/Vλ. Less aggregation of the pertuzumab Fab containing Cλ was observed compared to the pertuzumab scFv even though the improvement in Fv thermal stability (based on Tm) was weak. Additionally, the pertuzumab Fab with Cλ was stable without aggregating for >6 months in solution under refrigerated conditions. The pertuzumab VH/Vκ scFv did not express with an appreciable level of monomeric protein without being N-terminally fused to an Fc (some diabody may form, although this was not investigated). Adding the Cα/Cβ domains, which had little effect on thermal stability, also improved the expression and level of monomer compared to the scFv. Thus, while the CH1/Cκ domains impart a large thermal stability benefit to VH/Vκ, and possibly enable assembly and secretion of mAbs with low stability VH/Vκ domains, addition of *any* of the constant domains subunits (CH1/Cκ, CH1/Cλ, or Cα/Cβ) to VH/Vκ had a highly beneficial effect on monodispersity and expression. This may be biologically the more important role of the CH1/CL domains and of particular importance for CH1/Cλ where the unfolding cooperativity between constant and variable domain subunits is much weaker.

It could be hypothesized that the correct constant domain/variable domain pairings (e.g., CH1/Cκ with VH/Vκ) may be important for full activity. In fact, a study by Ponomarenko and coworkers showed that the Fab 'elbow angle' and domain dynamics changed considerably when replacing Cλ with Cκ in a naturally λ LC containing Fab.[27] This resulted in multiple CDR residues changing rotomer positions and subtle alterations in substrate specificity and catalytic efficiency of the catalytic antibody. We have not observed significant differences in antigen binding by replacing Cκ with Cλ[28] or CH1/Cκ with Cα/Cβ[17] having tested multiple Fabs with mismatched domains. It seems likely, as observed with scFvs, that subtle changes in affinity (2–4-fold) may occur when making unnatural variable and constant domain pairings, but that catastrophic changes in affinity/activity are likely not induced by modifying the constant domain subunits within Fabs.

It was interesting to note that VH/Vλ subunits were stable for all 6 λ LC containing antibodies that were evaluated (PGT128, 10C12, 3P6b_B01, and Antibody1λ-3λ). For even the less stable Fvs, the VH/Vλ subunits unfolded cooperatively, either in scFv or Fab formats. Such behavior was observed for only one of the 4 VH/Vκ scFvs described in this study. Folding cooperativity between VH and Vκ can be induced by engineering stronger interactions between VH and Vκ;[29] however, such cooperative unfolding appears not to be the norm. Two of the 4 VH/Vκ scFv described here formed significant aggregates (pertuzumab and Antibody1κ); whereas all 4 of the VH/Vλ scFvs were predominately monodisperse proteins with between 5–15% aggregates when expressed in mammalian cells. There was a trend for the scFvs with Vλ to be more stable (higher Tm). Such behavior may generally lead VH/Vλ scFvs to exhibit less aggregation and solubility issues than VH/Vκ scFvs.

Material and methods

Cloning, expression, and purification of Cκ, Cλ, C$_H$1/Cκ, and C$_H$1/Cλ

The constant domain sequences were obtained from the NCBI, synthesized by GeneArt, and subcloned into the pET21a (Cκ and Cλ) or pETDuet (CH1/Cκ and CH1/Cλ, Novagen). Ck and Cl protein sequences terminated just prior to the C-terminal cysteine and a C-terminal hexahistidine tag was added. CH1/Cκ and CH1/Cλ subunits both contained the C-terminal cysteines to enable formation of the interchain disulfide bond and a C-terminal hexahistidine tag on the CH1 domain. Plasmids were transformed into BL21-CodonPlus chemically competent cells (Agilent), inoculated into 1 L autoclaved luria broth media with either 100 μg/mL carb (pET21a) or 100 μg/mL carbenicillin/35 μg/mL kanamycin (pETDuet). Cultures were incubated at 37 °C shaking at 220 rpm until the cell culture density reached an $AU_{600\ nm}$ of ~1.5. At this point, 1 mM IPTG was added to induce protein expression, the culture temperature was reduced to 30 °C and allowed to continue for 4 hrs. Cultures were then collected and bacteria were pelleted by centrifugation at 4 g for 20 minutes. Protein was collected via periplasmic extraction of the bacteria from the pellet at ~5 °C using 50 mL of 100 mM Tris, 500 mM sucrose, 1 mM EDTA, and 100 μg/mL hen egg white lysozyme (Sigma) pH 8.0. The bacterial debris was then removed by centrifugation at 11 K rpm.

Purification of Cκ and Cλ was performed using anion exchange chromatography while CH1/Cκ and CH1/Cλ was performed using cation exchange chromatography. For the isolated Cκ and Cλ domains, the periplasmic extracts were diluted 1:10 into 10 mM Tris pH 9.0. Protein from these solutions was captured onto Q sepharose resin (GE Healthcare), washed with 10 mM Tris pH 9.0 and eluted using 10 mM Tris, 0.7 M NaCl, pH 9.0. For the CH1/Cκ and CH1/Cλ heterodimers, the periplasmic extracts were diluted 1:10 into 10 mM citrate, 10 mM NaCl pH 5.5. Protein from these solutions was captured onto SP FF resin (GE Healthcare), washed with 10 mM citrate, 10 mM NaCl pH 5.5 and eluted using 10 mM citrate, 10 mM NaCl, 0.7 M NaCl. The SP eluants were buffer exchanged into 50 mM Tris, pH 8.0. These ion exchange eluants were passed over a cobalt resin (Thermo), washed with 50 mM Tris, pH 8.0 and eluted using 20 mM imidazole, pH 8.0. Surprisingly, there was no need to go to higher concentrations of imidazole to elute the proteins.

Cloning, expression, and purification of varied scFv and Fab constructs

Oligonucleotides containing the Kappa, Lambda, and TCR constant domains were designed and amplified by PCR from existing in-house DNA templates.[17,28] All full gene constructs for subcloning were synthesized using PCR-based overlapping oligonucleotide synthesis or direct synthesis from Integrated DNA Technologies (IDT). The inserts were subcloned into a CMV promotor-driven mammalian expression vector (Lonza). Secretion was driven using a common mouse antibody LC signal sequence that is translated in-frame as part of the expressed protein and cleaved prior to secretion. Plasmid ligations, transformations, DNA preparations were performed using standard molecular biology protocols. For expression, LC and HC plasmids were co-transfected into HEK293F cells (1:1 ratio for the HC and LC with 1 μg DNA/uL cell culture) using Freestyle transfection reagents (Life Technologies). Transfected cells were grown at 37 °C in a 5% CO_2 incubator while shaking at 125 rpm. Secreted protein was harvested on day 5 by centrifugation for 5 min. Supernatants were passed through 2 μm filters (both large scale and small scale) for purification.

Small-scale (2 mL) purifications were performed by directly incubating transfected supernatants with 100 μL resuspended, phosphate-buffered saline (PBS)-washed His Pur™ Cobalt Resin bead (Thermo). Beads were washed 2-times with PBS, 20 mM imidazole according to the manufacturer's protocols. Protein was eluted from the beads by adding PBS, 300 mM Imidazole, PH 8.0. Large scale purifications were performed by passing the supernatants over a 5 mL HisTrap™ FF nickel affinity chromatography column using an AKTA Explorer (both from GE Healthcare). The nickel column was washed with 20 mM Tris HCl, 0.5 M NaCl, 20 mM Imidazole, PH 8.0, then proteins were eluted using 20 mM Tris HCl, 0.5 M NaCl, 300 mM Imidazole, PH 8.0. All proteins were concentrated, dialyzed against PBS, aliquoted, and stored at 4 °C until characterized. Enzymatic deglycosylation of the Cα/Cβ domains within the Cα/Cβ-containing pertuzumab Fab was performed using N-Glycanase® (ProZyme) according to the manufacturer's instructions.

Characterization of protein assembly and size

Proteins were initially characterized by SDS-PAGE and analytical SEC with in-line static light scattering. SDS-PAGE analyses were performed using Novex® 4–20% Tris Glycine gels or 3–8% Tris-Acetate gels according to manufacturer protocols (Life Technologies). Approximately 5 μg protein was loaded in each well and the SeeBluePlus2 (Life Technologies) molecular weight marker was used. Gels were stained with Novex SimplyBlue™ SafeStain (Life Technologies) and destained in water. Analytical SEC with in-line light scattering (SEC/LS) was performed by injecting 30–80 μL of each sample purified directly from 1 mL supernatants or after large-scale purification (concentrations ~0.2–0.8 mg/mL) onto a Sepax Zenix SEC 200 analytical HPLC (7.8×300 mm) column or a Phenomenex Yarra G3000 SEC analytical HPLC (7.8×300 mm) column equilibrated in 10 mM phosphate, 150 mM NaCl, 0.02% NaN3, pH 6.8, using an Agilent 1100 HPLC system. Static light scattering data for material eluted from the SEC column were collected using a miniDAWN TREOS static light scattering detector coupled to an Optilab T-rEX in-line refractive index meter (Wyatt Technologies). UV data were analyzed using HPCHEM (Agilent). Molecular weights of the proteins were determined by their static light scattering profiles using the ASTRA V software (Wyatt Technologies).

Chemical denaturations monitored by far UV Circular dichroism (CD)

The chemical stability of particular Fabs was measured by performing GuHCl titrations. Mixtures of protein sample, phosphate buffer, 8 M GuHCl at pH 7.0 were prepared to generate a GuHCl gradient (0–6 M) with constant protein concentration (1 mg/mL or 2 mg/mL). All samples in GuHCl were allowed to equilibrate for 3 d at 4 °C prior to taking Far UV CD spectra. CD spectra were collected at 20 °C in an automated Chirascan-Plus Circular Dichroism Spectrometer (Applied Photophysics Ltd, Leatherhead UK). Enough sample was prepared to sample from a sealed 96-well plate 3 separate times to generate the GuHCl denaturation curves. All curves were the average of 3 subsequent titrations. Far UV CD spectra were collected in the range of 195–250 nm using a 0.2 mm path length cuvette for each sample. The scanning step size was 1 nm with a sampling time of 1 s and bandwidth of 1 nm. Spectra were analyzed using the ProData Software provided by the manufacturer.

DSC measurements

DSC scans were performed using an automated capillary DSC (capDSC, MicroCal, LLC). Fab solutions (0.5–1 mg/mL protein in PBS) and PBS buffer were sampled automatically from 96-well plates using the robotic attachment. Prior to each protein scan, 2 buffer scans were performed to define the baseline for subtraction. All 96-well plates containing protein were stored within the instrument at 6 °C. Scans were performed from 20 to 105 °C at 2 °C/min using the low feedback mode. Subsequent to the subtraction of reference baseline scans, the baselines were further corrected by subtracting a third order polynomial. Analysis was performed using the Origin software supplied by the manufacturer.

ANS fluorescence

Fluorescence emission spectra were collected using a GEMINI EM microplate reader (Molecular Devices). ANS was from Sigma. Fluorescence measurements were performed using 40 μM ANS and 20 μM protein at room temperature in pH 7.0 and pH 2.0 buffers containing 10 mM phosphate and 20 mM Acetate, respectively. Neutral pH fluorescence spectra were taken for α-lactalbumin in a pH 8.0, 20 mM Tris, 0.5 mM $CaCl_2$ buffer. ANS excitation was performed at 375 nm. Emission spectra were recorded from 410–600 nm with a 1 nm step sizes. Both the excitation and emission bandwidths were 9 nm.

Disclosure of potential conflicts of interest

No potential conflicts of interest were disclosed.

Acknowledgments

We thank Benjamin Gutierrez for his help with transient transfections, Michael Bacica for intact mass spectrometry analyses, and Heather Austin and Carina Torres for antibody discovery efforts.

References

1. Ecker DM, Jones SD, Levine HL. The therapeutic monoclonal antibody market. mAbs 2015; 7:9-14; PMID:25529996; http://dx.doi.org/10.4161/19420862.2015.989042
2. Bork P, Holm L, Sander C. The immunoglobulin fold. Structural classification, sequence patterns and common core. J Mol Biol 1994; 242:309-20; PMID:7932691.
3. Feige MJ, Buchner J. Principles and engineering of antibody folding and assembly. Biochim Biophys Acta 2014; 1844:2024-31; PMID:24931831; http://dx.doi.org/10.1016/j.bbapap.2014.06.004
4. Vermeer AW, Norde W. The thermal stability of immunoglobulin: unfolding and aggregation of a multi-domain protein. Biophys J 2000; 78:394-404; PMID:10620303; http://dx.doi.org/10.1016/S0006-3495(00)76602-1
5. Garber E, Demarest SJ. A broad range of Fab stabilities within a host of therapeutic IgGs. Biochem Biophys Res Commun 2007; 355:751-7; PMID:17321501; http://dx.doi.org/10.1016/j.bbrc.2007.02.042
6. Harn N, Allan C, Oliver C, Middaugh CR. Highly concentrated monoclonal antibody solutions: direct analysis of physical structure and thermal stability. J Pharm Sci 2007; 96:532-46; PMID:17083094; http://dx.doi.org/10.1002/jps.20753
7. Demarest SJ, Glaser SM. Antibody therapeutics, antibody engineering, and the merits of protein stability. Curr Opin Drug Discov Devel 2008; 11:675-87; PMID:18729019
8. Rothlisberger D, Honegger A, Pluckthun A. Domain interactions in the Fab fragment: a comparative evaluation of the single-chain Fv and Fab format engineered with variable domains of different stability. J Mol Biol 2005; 347:773-89; PMID:15769469; http://dx.doi.org/10.1016/j.jmb.2005.01.053
9. Brandts JF, Hu CQ, Lin LN, Mos MT. A simple model for proteins with interacting domains. Applications to scanning calorimetry data. Biochemistry 1989; 28:8588-96; PMID:2690944; http://dx.doi.org/10.1021/bi00447a048
10. Demarest SJ, Chen G, Kimmel BE, Gustafson D, Wu J, Salbato J, Poland J, Elia M, Tan X, Wong K, Short J, Hansen G. Engineering stability into Escherichia coli secreted Fabs leads to increased functional expression. Protein Eng Des Sel 2006; 19:325-36; http://dx.doi.org/10.1093/protein/gzl016
11. Michaelson JS, Demarest SJ, Miller B, Amatucci A, Snyder WB, Wu X, Huang F, Phan S, Gao S, Doern A, et al. Anti-tumor activity of stability-engineered IgG-like bispecific antibodies targeting TRAIL-R2 and LTbetaR. mAbs 2009; 1:128-41; PMID:20061822; http://dx.doi.org/10.4161/mabs.1.2.7631
12. Jefferis R, Deverill I, Ling NR, Reeves WG. Quantitation of human total IgG, kappa IgG and lambda IgG in serum using monoclonal antibodies. J Immunol Methods 1980; 39:355-62; PMID:6780626; http://dx.doi.org/10.1016/0022-1759(80)90235-5
13. Matsunaga T, Tormanen V. Evolution of antibody and T-cell receptor V genes–the antibody repertoire might have evolved abruptly. Dev Comp Immunol 1990; 14:1-8; PMID:2338149; http://dx.doi.org/10.1016/0145-305X(90)90002-V
14. Franklin MC, Carey KD, Vajdos FF, Leahy DJ, de Vos AM, Sliwkowski MX. Insights into ErbB signaling from the structure of the ErbB2-pertuzumab complex. Cancer Cell 2004; 5:317-28; PMID:15093539; http://dx.doi.org/10.1016/S1535-6108(04)00083-2
15. Pejchal R, Doores KJ, Walker LM, Khayat R, Huang PS, Wang SK, Stanfield RL, Julien JP, Ramos A, Crispin M, et al. A potent and broad neutralizing antibody recognizes and penetrates the HIV glycan shield. Science 2011; 334:1097-103; PMID:21998254; http://dx.doi.org/10.1126/science.1213256
16. Goo L, Jalalian-Lechak Z, Richardson BA, Overbaugh J. A combination of broadly neutralizing HIV-1 monoclonal antibodies targeting distinct epitopes effectively neutralizes variants found in early infection. J Virol 2012; 86:10857-61; PMID:22837204; http://dx.doi.org/10.1128/JVI.01414-12
17. Wu X, Sereno AJ, Huang F, Zhang K, Batt M, Fitchett JR, He D, Rick HL, Conner EM, Demarest SJ. Protein design of IgG/TCR chimeras for the co-expression of Fab-like moieties within bispecific antibodies. mAbs 2015; 7:364-76; PMID:25611120; http://dx.doi.org/10.1080/19420862.2015.1007826
18. Demarest SJ, Frasca V. Differential Scanning Calorimetry in the Biopharmaceutical Sciences, In Biophysical Characterization of Proteins in Developing Biopharmaceuticals (Houde DJ, Berkowitz SA, Ed.) 2014; pp 287-306, Elsevier B.V.
19. Feige MJ, Groscurth S, Marcinowski M, Shimizu Y, Kessler H, Hendershot LM, Buchner J. An unfolded CH1 domain controls the assembly and secretion of IgG antibodies. Mol Cell 2009; 34:569-79; PMID:19524537; http://dx.doi.org/10.1016/j.molcel.2009.04.028
20. Holt LJ, Herring C, Jespers LS, Woolven BP, Tomlinson IM. Domain antibodies: proteins for therapy. Trends Biotechnol 2003; 21:484-90; PMID:14573361; http://dx.doi.org/10.1016/j.tibtech.2003.08.007
21. Borbulevych OY, Santhanagopolan SM, Hossain M, Baker BM. TCRs used in cancer gene therapy cross-react with MART-1/Melan-A tumor antigens via distinct mechanisms. J Immunol 2011; 187:2453-63; http://dx.doi.org/10.4049/jimmunol.1101268
22. Chen JL, Stewart-Jones G, Bossi G, Lissin NM, Wooldridge L, Choi EM, Held G, Dunbar PR, Esnouf RM, Sami M, et al. Structural and kinetic basis for heightened immunogenicity of T cell vaccines. J Exp Med 2005; 201:1243-55; PMID:15837811; http://dx.doi.org/10.1084/jem.20042323
23. Semisotnov GV, Rodionova NA, Razgulyaev OI, Uversky VN, Gripas AF, Gilmanshin RI. Study of the "molten globule" intermediate state in protein folding by a hydrophobic fluorescent probe. Biopolymers 1991; 31:119-28; PMID:2025683; http://dx.doi.org/10.1002/bip.360310111
24. Kuwajima K. The molten globule state of α-lactalbumin. FASEB J 1996; 10:102-9; PMID:8566530
25. Huang M, Furie BC, Furie B. Crystal structure of the calcium-stabilized human factor IX Gla domain bound to a conformation-specific anti-factor IX antibody. J Biol Chem 2004; 279:14338-46; PMID:14722079; http://dx.doi.org/10.1074/jbc.M314011200
26. Chodorge M, Zuger S, Stirnimann C, Briand C, Jermutus L, Grutter MG, Minter RR. A series of Fas receptor agonist antibodies that demonstrate an inverse correlation between affinity and potency. Cell Death Differ 2012; 19:1187-95; PMID:22261618; http://dx.doi.org/10.1038/cdd.2011.208
27. Ponomarenko N, Chatziefthimiou SD, Kurkova I, Mokrushina Y, Mokrushina Y, Stepanova A, Smirnov I, Avakyan M, Bobik T, Mamedov A, et al. Role of kappa–>lambda light-chain constant-domain switch in the structure and functionality of A17 reactibody. Acta Crystallogr D Biol Crystallogr 2014; 70:708-19; http://dx.doi.org/10.1107/S1399004713032446
28. Lewis SM, Wu X, Pustilnik A, Sereno A, Huang F, Rick HL, Guntas G, Leaver-Fay A, Smith EM, Ho C, et al. Generation of bispecific IgG antibodies by structure-based design of an orthogonal Fab interface. Nat Biotechnol 2014; 32:191-8; PMID:24463572; http://dx.doi.org/10.1038/nbt.2797
29. Miller BR, Demarest SJ, Lugovskoy A, Huang F, Wu X, Snyder WB, Croner LJ, Wang N, Amatucci A, Michaelson JS, Glaser SM. Stability engineering of scFvs for the development of bispecific and multivalent antibodies. Protein Eng Des Sel 2010; 23:549-57; http://dx.doi.org/10.1093/protein/gzq028
30. Myers JK, Pace CN, Scholtz JM. Denaturant m values and heat capacity changes: relation to changes in accessible surface areas of protein unfolding. Protein Sci 1995; 4:2138-48; PMID:8535251; http://dx.doi.org/10.1002/pro.5560041020